DOI: 10.1002/ejic.201000561

Crystal Structures and Magnetic Properties of Newly Synthesized Mono- and Dinuclear Cu^{II} Schiff-Base Complexes

Snehadrinarayan Khatua,[a] Jina Kang,[a] Kibong Kim,[a] Jung Oh Huh,[b] Junseong Lee,[b] Chang Seop Hong,[c] and David G. Churchill*[a]

Dedicated to Professors Youngkyu Do and Joon Taik Park on the occasion of their 60th birthdays

Keywords: Copper / Schiff bases / Magnetic properties / Hydrogen bonds

Five Cu^{II} Schiff-base complexes, three mononuclear {[Cu(*rslys*H)·$(H_2O)_2$]·$2H_2O$·ClO_4 (**1**); [Cu(*rslys*H)Cl] (**2**); [Cu(*slys*H)(H_2O)Cl] (**3**) *rslys* and *slys* = 6-amino-2-[(2-hydroxybenzylidene)amino]hexanoate} and two dinuclear {[Cu_2(*rslys*H)$_2$$(CH_3OH)_2$]·$(H_2O)_2(NO_3)_2$ (**4**); [Cu_2(*slys*H)$_2$-$(NO_3)_2$]·$(H_2O)_3$ (**5**)}, are reported herein. These complexes have been synthesized via a facile "one-pot" method in which the D/L- and L-lysine Schiff-base ligands are generated in situ. Various spectroscopic techniques and single-crystal X-ray diffraction were used in compound characterization. The X-ray diffraction studies revealed that complexes **1**–**3** are mononuclear; further, **4** and **5** are dinuclear in which two Cu^{II} centers are phenolate-bridged. Complexes **1**, **2** and **3** are structurally similar, according to the nuclearity and the coordination environment around the metal center involving a tridentate D- or L-lysine-derived Schiff-base ligand. But the crystallographic packing is different, owing to the different counterions and number of solvent molecules present in the crystals. Compounds **1** and **2** are racemic due to the co-existence of chiral D- and L-lysine-based Schiff-base ligands. These copper(II) complexes give 2-D hydrogen-bonded networks and are racemic overall. Compound **3** is chiral, containing only the L-lysine-derived ligand in which a cylindrical 1-D hydrogen-bonded structure is observed in the solid state. Both **4** (achiral) and **5** (chiral) reveal 3-D hydrogen-bonded networks. A strong antiferromagnetic coupling interaction was observed by variable-temperature magnetic susceptibility measurements; this interaction is likely mediated through the phenolate bridge between the two Cu^{II} centers in **4** and **5**.

Introduction

Copper(II) chemistry in biology research commonly relates to chelation, chaperones and oxidative stress (Fenton Chemistry).[1,2,3a] How this extremely well-studied metal ion undergoes complexation with simple natural ligands (amino acids) is greatly, but not exhaustively, explored. Further, the possibility of Schiff-base formation in biology that enables artificial metal binding sites is an interesting, and relatively unexplored area. The culprits that enable Schiff-base formation might be many, but reactive aldehydes which can functionalize pendant amines (lysine side chains, etc) are often pointed to. While there are various natural aldehydes [e.g., 3-aminopropanal, 4-hydroxynonenal (HNE), 4-hydroxy-2-hexenal (HHE), 4-oxo-2-nonenal (ONE), acrolein], the utility of using salicylaldehyde in model studies facilitates various properties such as compound rigidity, crystallinity, and enables optical properties but does have limitations. Thus in this study we wish to explore facile in situ imine formation with Cu^{2+} and lysine (two naturally-occurring species) with salicylaldehyde in forming Schiff-base complexes. Salicylaldehyde is also natural,[3b] but perhaps less encountered in human health.

Inherent in this research, from a materials perspective, is the facile approach for the preparation of new *chiral* metal complexes. The involvement of amino acid starting materials allows for a natural stereogenic center. Here, strong donor groups like the phenoxyl oxygen atom (Ar-*O*) and imine nitrogen atoms (RR′C=*N*–R′′) due to the wide range of applications and structural aspects of the resulting transition metal complexes.[4] This tridentate ligand allows for the formation of mono- and dinuclear species. We can also explore the crystalline details of these closely related species and how magnetochemistry manifests in these discrete com-

[a] Molecular Logic Gate Laboratory, Department of Chemistry, Korea Advanced Institute of Science and Technology (KAIST) 373-1 Guseong-dong, Yuseong-gu, Daejeon, 305-701, Republic of Korea
Fax: +82-42-350-2810
E-mail: dchurchill@kaist.ac.kr
[b] Molecular Materials Laboratory, Department of Chemistry, Korea Advanced Institute of Science and Technology (KAIST), 373-1 Guseong-dong, Yuseong-gu, Daejeon, 305-701, Republic of Korea
[c] Department of Chemistry and Centre for Electro- and Photo-Responsive Molecules, Korea University, Seoul, 136-701, Republic of Korea

Supporting information for this article is available on the WWW under http://dx.doi.org/10.1002/ejic.201000561.

plexes.[5] This does not relate centrally to oxidative stress and neurodegenerative diseases, but such features also allow for a fuller understanding of the potential physical properties of these simply-prepared compounds. While there are some articles relating to such Cu^{2+} amino acid-based Schiff-base complexes, or their reduced versions, we can look into intermolecular arrangements, with emphasis on hydrogen bonding.[6] Noncovalent atomic interactions are widely observed in many materials, and exploited in respective natural and synthetic supramolecular chemical systems. Hydrogen bonding, π-stacking, as well as electrostatic, hydrophobic and charge-transfer interactions can dictate chiral motifs in solids. Biological applications such as antibacterial, antiviral, antifungal species and DNA cleaving agents could later be addressed.[7] Also, chiral copper complexes have been exploited for use in asymmetric catalysis of organic transformations such as olefin polymerization/enantioselective epoxidation, asymmetric hetero-Diels Alder reactions, etc.[8]

Herein, we discuss the synthesis, structure and solution properties of five Cu^{II} Schiff-base complexes, three mononuclear (**1**–**3**) and two dinuclear ones (**4** and **5**). Extended 2-D and 3-D hydrogen-bonded interactions are considered here. A discussion of the magnetic properties of compounds **4** and **5** is also included.

Results and Discussion

Synthesis and Characterization of Chiral/Achiral Mono- and Dinuclear Cu^{II} Schiff-Base Complexes

Mono- and dinuclear copper complexes of L-lysine-based Schiff-base ligands (Scheme 1) were synthesized in a "one-pot" method. The Schiff-base ligands (D- and L-lysine-based ligands) were formed in situ (Scheme 1). The synthetic scheme is analogous to that of the dinuclear zinc and copper complexes recently reported by this research group.[9] The aqueous solution of copper salts were added to a methanolic salicylaldehyde solution, followed by the addition of an aqueous solution of D/L or L-lysine. An aqueous NaOH solution was then added dropwise into the reaction mixture; finally a few drops of triethylamine were added to the reaction mixture to maintain a pH value of about 7.0 where needed (Et_3N was used for compound **1**–**3**). After allowing 12 hours for reaction, a slow evaporation of the reaction mixture gave a blue (compound **1**), dark blue (**2**) and dark green (**3**–**5**) material (depending on the starting material). The quality of these crystalline products enabled immediate specimens for single-crystal X-ray diffraction. These compounds were also characterized by elemental analyses, IR, UV/Vis, ESI-MS, and CD spectroscopy. An aqueous $NaNO_3$ solution was used during the synthesis of compound **4** to prevent the formation of mononuclear compound **2** as a side product.

Solution Properties of Mono- and Dinuclear Cu^{2+} Compounds

The solution properties of complexes **1**–**3** and **4**–**5** were studied by UV/Vis, circular dichroism (CD) (for **3** and **5** only) and ESI-MS. The UV/Vis spectra of compounds **1**–**5** were recorded in aqueous solution at room temperature which show intense peaks at ca. 357 nm, 267 nm and 238 nm assigned to the LMCT and *intra*-ligand charge transfer transitions, respectively. The broad band at 500–800 nm seen in concentrated (100 μM) solution was assigned to the d–d transition (Figures S1–S5, Supporting Information). The ESI-MS of compounds **1**–**5** were collected in a water/methanol mixture. The spectra of these compounds clearly show a 100% positive ion peak at 312.059 and 623.095 for cations of **1** and **4**, respectively, and negative ion peaks at 346.018, 684.076 for anions of **2**, **3** and **5** (Fig-

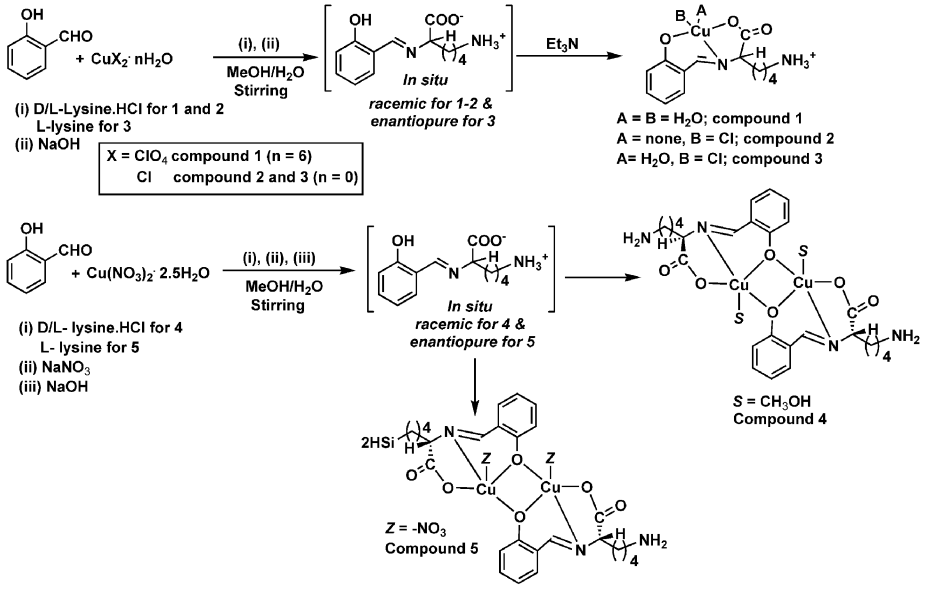

Scheme 1. Synthesis of copper complexes **1**–**5**.

ures S6–S11, Supporting Information), respectively. These results suggest that, not only mononuclear complexes **1**–**3**, but also, phenolate-bridged dinuclear complexes **4** and **5** are stable in solution.

Both compounds **3** and **5** are chiral due to the presence of L-lysine residues as part of the Schiff-base ligand. The solution CD spectra of compounds **3** and **5** were collected in water at 25 °C. The spectra of both compounds are very similar and reveal negative Cotton effects at about 360 (358), ca. 276 nm, and a positive effect at about 238 nm (Figure 1).

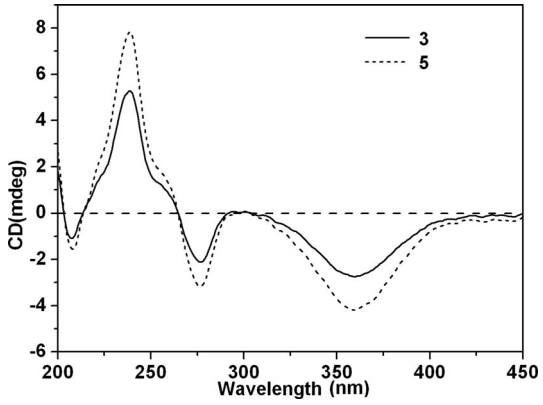

Figure 1. Solution circular dichroism (CD) spectra of compounds **3** and **5** (cell path length: 1 cm).

X-ray Crystallography

The molecular structures of compounds **1**–**3** are shown in Figure 2 (a–c); those of compounds **4** and **5** are shown in Figure 4 (a and b), respectively. Single-crystal X-ray diffraction analysis reveals that complexes **1**, **2** and **4** crystallize in the centrosymmetric space groups $P\bar{1}$, $P2_1/c$ and $P\bar{1}$, respectively, whereas compounds **3** and **5** are found in the chiral noncentrosymmetric space groups $P2_12_12_1$ and C_2.

Molecular Structures of [Cu(rslysH)·(H$_2$O)$_2$]·ClO$_4$·2H$_2$O (1), [Cu(rslysH)Cl] (2) and [Cu(slysH)(H$_2$O)-Cl] (3): The structures of compounds **1**–**3** show that they are discrete and mononuclear (Figure 2). In **1**, the metal center, assigned as copper, is bonded by the tridentate Schiff-base ligand. Two water molecules complete a slightly distorted square-pyramidal coordination geometry; this minor shift from ideality is defined by the distortion parameter (τ). The tau-descriptor (τ) for five coordinated complexes is expressed as the difference between the two *trans* angles O(1)–Cu(1)–O(2) and N(1)–Cu(1)–O(1 W) (Table 1) divided by 60 gives a value of 0.15; the ideal values are 1 for a trigonal bipyramid and 0 for a square pyramid.[10] The terminal –NH_2 group of the Schiff-base ligand is protonated and the charge is balanced by the perchlorate counterion.[11] In compound **2**, the metal center, assigned as copper adopts a square-planar geometry and is bonded by the [O_2N] donor atoms of the Schiff-base ligand, and a chloride ligand. Here, complex electroneutrality of the copper(II) species is satisfied by the protonation of the terminal amine group (–NH_3^+). It is noteworthy that the racemic D/L lysine hydrochloride was used in the synthesis of compounds **1** and **2**. The crystal structures contain both optical isomeric complexes (complex with D-lysine-based Schiff-base ligand as ***D*** and L-lysine-based ligand as ***L***) and the compound becomes racemic. The structure of complex **3** is different from that of compound **2** where the copper center is axially bonded to a water oxygen atom allowing for a distorted square pyramidal geometry (τ parameter: 0.215).

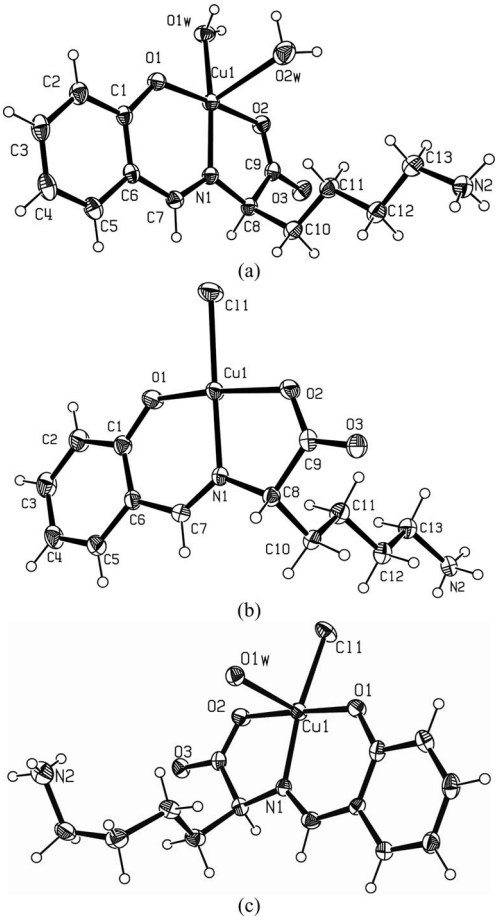

Figure 2. Crystal structures of compounds (a) **1**, (b) **2** and (c) **3**. The solvent water molecule and disordered ClO_4^- ion are omitted for clarity from the molecular drawing of compound **1**. Thermal ellipsoids are drawn at 30% probability level.

In these compounds, the observed extended 1-D to 3-D networks are due to hydrogen bonding. In **1**, there are two water molecules present in the unit cell. With the help of these water solvent molecules of crystallization and the perchlorate counterion, a 3-D hydrogen-bonded network is able to exist (Figure 3, a). Since both the D- and L-lysine-based Schiff-base copper complexes (***D*** and ***L***) are present in the crystal, the network taken in its entirety is racemic (Figure 3, a). In **2**, the carboxylate oxygen, O3 forms a hydrogen bond with terminal amine hydrogen atoms [N2^a–H2N···O3 2.874(3) Å, N2^b–H3N···O3 2.827(3) Å where a =

–1 + *x*, *y*, *z* and b = 2 – *x*, 1 – *y*, 1 – *z*] of two adjacent complex and the copper-bound chloride forms a 2-D sheet. As in the crystalline matrix of compound **1**, here also the network is racemic because of the presence of both the ***D*** and ***L*** isomeric complexes in the crystal lattice. In compound **3**, a hydrogen-bonded 1-D cylindrical structure is observed. The cylindrical structure consists of a 1-D water–oxygen chain that can be interpreted as a left-handed helix when considering the interactions O1W···O3^{c} [2.81(5) Å], O3^{c}···O1W^{d} [2.81(5) Å] and O1W^{d}···O3 [2.71(5) Å] hydrogen bonding distances; this runs along the crystallographic *a* axis. The cylindrical structure is formed due to the N1–H2NC···O1W [3.24(6) Å], N2–H2NB···O1 [3.02(6) Å] and N2–H2NA···Cl [3.32(6) Å] hydrogen bonds (Figure 3, c).

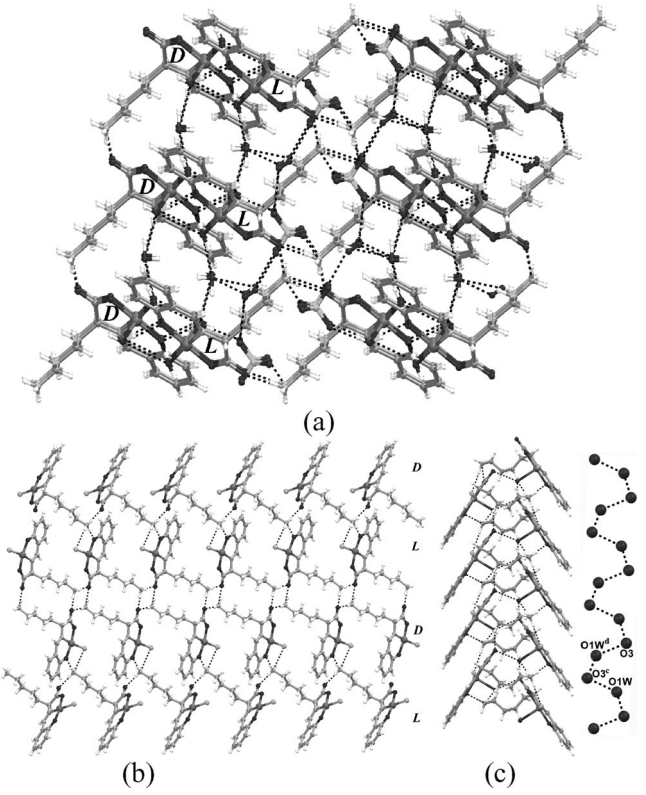

Figure 3. (a) View of the 3-D hydrogen-bonded network for compound **1** along the *b*-axis. (b) The hydrogen-bonded 2-D structure in compound **2**. (c) View of the hydrogen-bonded cylindrical structure in compound **3** in which exclusive mapping of the coordinated water molecule oxygen atoms forms a left handed helical chain with the help of carboxylate oxygen. [symmetry codes, c: –1/2 + *x*, 1/2 – *y*, 2 – *z*; d: 1/2 + *x*, 1/2 – *y*, 2 – *z*].

Structure of [Cu$_2$(rslysH)$_2$(CH$_3$OH)$_2$]·(H$_2$O)$_2$(NO$_3$)$_2$ (4) and [Cu$_2$(slysH)$_2$(NO$_3$)$_2$]·(H$_2$O)$_3$ (5): Compounds **4** and **5** are dinuclear (Figure 4). Compound **4** is racemic as it consists of both the D- and L-lysine-based Schiff-base ligand. Whereas, compound **5** is chiral as it involves a L-lysine-based moiety. In **4**, the copper centers are in a slightly distorted square pyramidal arrangement through the tridentate [O_2N] atom donor Schiff-base ligand coordination. The 4th *basal* position is occupied by the bridging phenolate oxygen. The *axial* position is occupied by a solvent molecule assigned and least-squares refined as methanol. The copper deviated around 0.22 Å above its basal plane. The tau (τ) parameter is 0.11 which also suggests a distorted square pyramidal arrangement. From the C_i symmetric core structure, an appreciation can be made of two square pyramids joined by a basal edge. This is in contrast with **5**, discussed next.

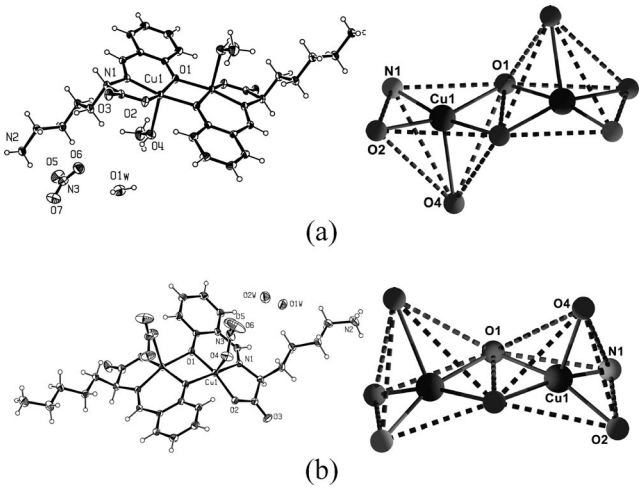

Figure 4. Crystal structures of compounds **4** and **5**. Thermal ellipsoids are drawn at 30% probability level.

The structure of compound **5** is similar with a previously reported dinuclear zinc compound from this laboratory.[12] In **5**, the copper centers are in a slightly distorted square pyramidal geometry (τ parameter: 0.04) by a coordinating tridentate Schiff-base ligand and one bridging phenolate oxygen. Unlike **4**, in this complex, the axial position is occupied by the nitrate anion. The core structure of this complex clearly allows for an interpretation of the coordination polyhedron as two square pyramids that share an edge; the axial nitrate ligands are present on the same side of the dimer. The phenolate-bridged dimer is C_2 symmetric. The features of compound **5** are more rare compared to those of compound **4**. As mentioned before in our previous reports, only a few closely-related copper dimers are known [including our previously reported lysine-derived copper(II) Schiff-base complex **1**, ref.[8f]]. These involve reduced Schiff-base ligands which bear close structural similarity to those here.[13]

In **4**, due to the presence of several hydrogen-bond donors (–NH_3^+, solvent H_2O, –OH of coordinated methanol) and acceptors [carbonyl, >C=O, and carboxylate oxygen, –C(O)O$^-$, and nitrate, –NO_3^-] extended hydrogen-bonded networks are observed. The carbonyl oxygen atoms, O3 form hydrogen bonds with H2Na of the terminal –NH_3^+ group of the neighbouring dimeric complex; a 1-D chain is formed along the crystallographic *a* axis [N2^{e}–H2Na^{e}···O3 2.86(18) Å, symmetry code e: *x*, 1 + *y*, *z*]. The solvent water molecule O1W acts as a hydrogen-bond donor in an interaction with an oxygen (O5^{e}) of one and another nitrate ion

(O6[f]) [O1W–H1Wa···O5[e] 3.01(3) Å and O1W–H1Wb···O6[f] 2.95(3) Å; symmetry code f: –*x*, 1 – *y*, 1 – *z*]. The oxygen O6 again is bonded with the hydrogen of the hydroxy oxygen O4[g] of the coordinated methanol [O4[g]–H1O[g]···O6 2.862(3) Å; symmetry code g: –1 + *x*, *y*, *z*]; a 2-D network is thus formed (Figure 5, a). In **4**, the carbonyl oxygen O3 and the solvent water O1W accept into hydrogen bonding atoms H2Nb[h] and H2Nc[h] of the neighbouring 2-D sheets; this forms hydrogen-bonded 3-D networks [N2[h]–H2Nb[h]···O3 2.78(19) Å, N2[h]–H2Nc[h]···O1W[h] 2.906(3) Å; symmetry code h: 1 – *x*, –*y*, 3 – *z*] (Figure 5, b).

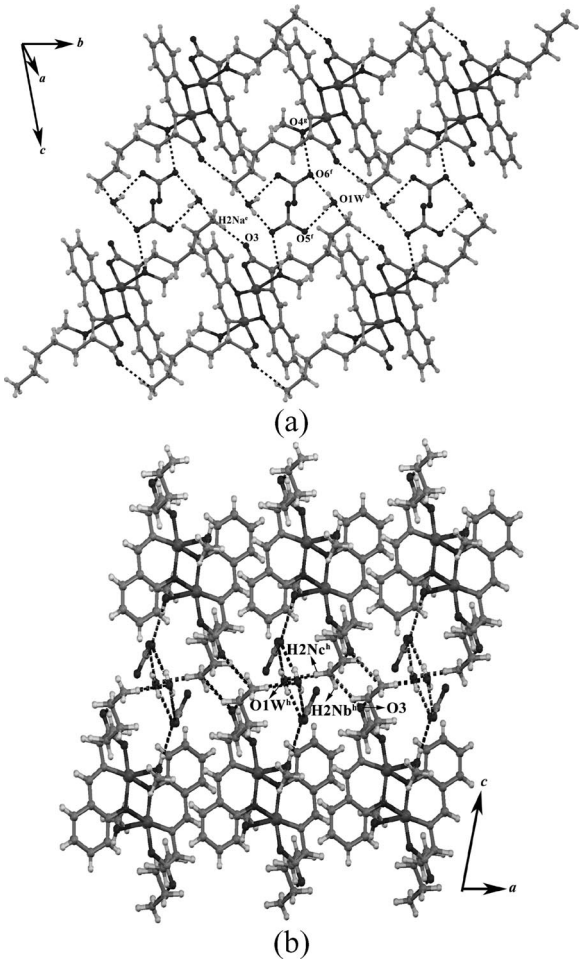

Figure 5. Representation of the hydrogen-bonded 2-D network and 3-D network in compound **4** (a) along the crystallographic *a* and (b) *b* axes [symmetry codes, e: *x*, 1 + *y*, *z*; f: –*x*, 1 – *y*, 1 – *z*; g: –1 + *x*, *y*, *z*; h: 1 – *x*, –*y*, 3 – *z*].

In **5**, the nitrates are bonded to the copper center through one oxygen atom (O5). The other oxygens O6 and O6[i] from the two nitrate groups form hydrogen bonds with the H2B[j] and H2B[k] of the terminal amine group (–NH_3^+) of the adjacent dimeric complexes [N2[j]–H2B[j]···O6; N2[k]–H2B[k]···O6[i] 2.92(8) Å; where, i: –*x*, *y*, 1 – *z*; j: –½ + *x*, –½ + *y*, *z*, and k: ½ + *x*, –½ + *y*, 1 – *z*]. As a result, a 2-D hydrogen-bonded network is formed (Figure 6, a). The two adjacent 2-D sheets are joined by the solvent water molecule O1W to give O1W···O2 and O1W···O2[l] [2.87(5) Å, with symmetry code l: –*x*, *y*, *z*] hydrogen bonding spans. Another water molecule O2W forms a hydrogen bond with one terminal –NH_3^+ hydrogen (H2C) of one 2-D sheet and carbonyl oxygen O3[m] of the adjacent 2-D sheet [N2–H2C···O2W 2.83(7) Å, O2W···O3[m] 3.03(7) Å, with m: ½ – *x*, –½ + *y*, 1 – *z*] and assists in the formation of a 3-D hydrogen-bonded network (Figure 6, b).

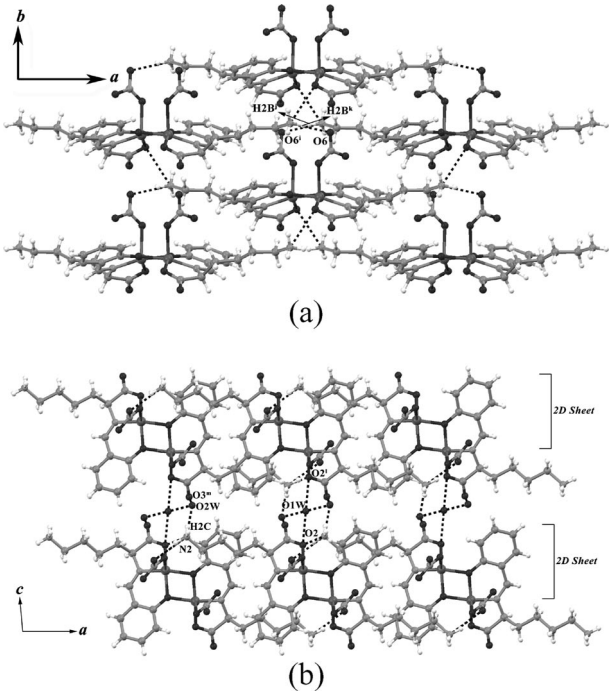

Figure 6. View of the hydrogen-bonded (a) 2-D network in compound **5** along the crystallographic *b*-axis and a (b) 3-D network as viewed along the crystallographic *c*-axis [symmetry code: i: –*x*, *y*, 1 – *z*; j: –½ + *x*, –½ + *y*, *z*; k: ½ + *x*, –½ + *y*, 1 – *z*; l: –*x*, *y*, *z*; m: ½ – *x*, –½ + *y*, 1 – *z*].

Magnetic Properties

The magnetic data for compounds **4** and **5** were recorded at 1 T as a function of temperature ranging from 4 to 300 K (Figure 7). The M(H) data for **4** was illustrated in Figure S12, still showing linear behaviour at 1 T. The drastic decrease in $\chi_m T$ is characteristic of strong antiferromagnetic interactions. The magnetic coupling constant between Cu^{II} ions through ligand bridging was estimated by employing a dimer model on the basis of the spin Hamiltonian $H = -JS_1 \cdot S_2$. The molecular field approximation was taken into account to include intermolecular magnetic interactions (z*J*′), and a fraction of noncoupled species (ρ) and temperature-independent paramagnetism (TIP) were also applied in the fitting process. The equation was expressed as follows.

$$\chi = (2Ng^2\beta^2/kT)/[3 + \exp(-J/kT)](1 - \rho) + \rho(Ng^2\beta^2/2kT) + \text{TIP}$$

$$\chi_m = \chi/(1 - zJ'\chi/Ng^2\beta^2)$$

A least-squares fit gives magnetic parameters of $g = 2.0$, $J = -401\ cm^{-1}$, $zJ' = -14.9\ cm^{-1}$, $\rho = 0.15$, TIP = $460 \times 10^{-6}\ cm^3\ mol^{-1}$ for compound **4**, and a least-squares

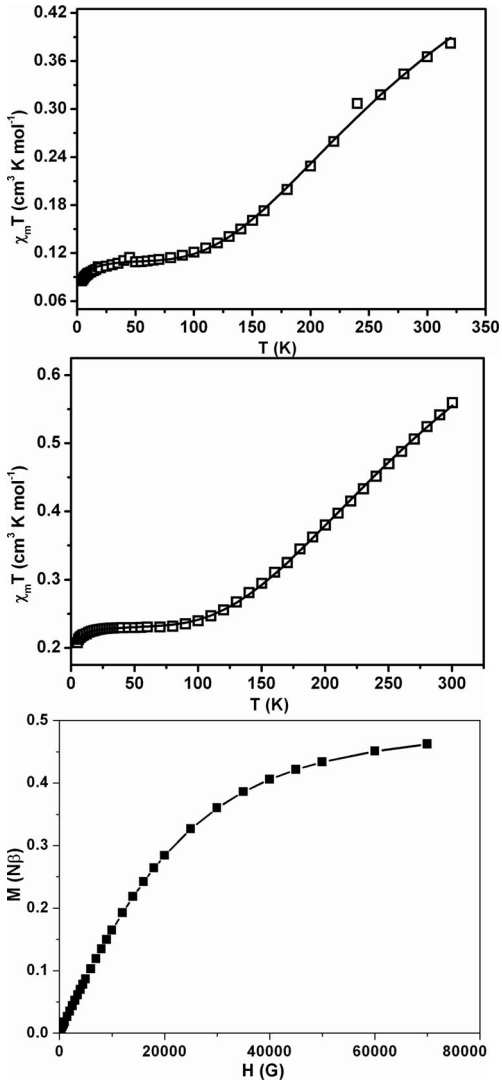

Figure 7. Top: Plot of $\chi_m T$ vs. T for compound **4** and compound **5** (middle). The solid trend lines represent a "best fit" of the given data points. Bottom: Field dependence of magnetization of **4** at 2 K.

fit gives magnetic parameters of g = 2.36, J = –416 cm^{-1}, zJ′ = –3.4 cm^{-1}, ρ = 0.22, TIP = 600 × 10^{-6} cm^3 mol^{-1} for compound **5**.[14] The curve fits the experimental data well (Figure 4, top: compound **4**; bottom: compound **5**). The J value obtained is in good agreement with those of Cu^{II} dimers with square pyramidal geometries.[15] The strong antiferromagnetic coupling is due to the effective orbital overlap between magnetic $d_{x^2-y^2}$ orbitals oriented along the Cu–$O_{phenoxide}$ vectors. The magnetic nature of this complex with the Cu–O–Cu angle of 101.3° corresponds to the prediction of magnetic behaviours in hydroxo-bridged Cu^{II} dimeric systems in which antiferromagnetic interactions occur at α > 97.5°.[16] The interdimer interactions (zJ′) are likely communicated via hydrogen bonds.

Conclusions

In this report, several new copper complexes were synthesized with ease (one-pot type reaction) and isolated in significant purity to allow for spectroscopic and single-crystal X-ray diffraction studies. The synthesis involved an easy one-pot method in which the Schiff-base ligands were formed in situ. The existing results give some interesting structural features. Among these compounds, compounds **1** and **2** are racemic due to the co-existence of both the D- and L-lysine-based Schiff-base copper(II) complex in their crystal lattice; the resulting 2-D hydrogen-bonded networks were interpreted as being racemic. Compound **3** is chiral, containing only a L-lysine-based Schiff-base copper(II) complex; a 1-D cylindrical hydrogen-bonded structure is observed in the solid state. Both complexes **4** and **5** are dinuclear, but complex **4** is achiral (*meso*) consisting of both the D- and L-lysine-based Schiff-base ligand, while complex **5** is chiral. Solution CD spectra were obtained in 100% aqueous media to demonstrate the chiral nature of compounds **3** and **5**. Extended hydrogen-bonded achiral and chiral 3-D networks were observed in **4** and in **5**, respectively. The variable temperature magnetic susceptibility measurements revealed that a strong antiferromagnetic coupling interaction exists, likely mediated through the phenolate bridge between the two Cu^{II} centers in compounds **4** and **5**.

Experimental Section

Materials and Physical Measurements: All chemicals used herein were used as received from commercial suppliers (Aldrich and TCI companies). Absorption spectra were measured using a JASCO V-530 UV/Vis spectrophotometer. Solution CD spectra were carried out with a JASCO-815 CD spectropolarimeter in aqueous solution. Elemental analyses were performed with a Vario EL III CHNS elemental analyzer. ESI-MS was performed in Bruker micrOTOF II mass spectrometer. Magnetic susceptibilities for **4** and **5** were measured on warming mode using a Quantum Design SQUID susceptometer. Diamagnetic corrections of **4** and **5** were estimated from Pascal's Tables and sample holder effect was corrected.

[Cu(*rslys*H)·(H$_2$O)$_2$]·2H$_2$O·ClO$_4$ (1): An aqueous solution of CuClO$_4$·6H$_2$O (1.85 g, 5.00 mmol) was added to a methanolic solution of salicylaldehyde (0.5 mL, 5.0 mmol). The reaction mixture became light green. After 30 min stirring at room temperature, an aqueous solution of D/L-lysine hydrochloride (0.91 g, 5.0 mmol) was added dropwise to the reaction mixture, followed by the successive slow addition of a portion of an aqueous NaOH solution (0.2 g, 5 mmol). A dilute methanolic solution of Et$_3$N (0.7 mL, 5 mmol) was then added to the reaction mixture which was maintained at a pH of 7–8. The reaction mixture turned dark blue-green. The stirring was maintained for a further 12 h. The reaction mixture was then filtered and kept for crystallization. Bluish crystals were then filtered and dried; yield (crystal) 73% (1.76 g). C$_{13}$H$_{25}$N$_2$O$_{11}$ClCu (M = 484.34 g mol^{-1}): calcd. C 32.24, H 5.20, N 5.78; found C 32.32, H 5.21, N 5.85. UV/Vis [λ_{max}/nm (ε/M^{-1} cm^{-1})] (H$_2$O): 357 (4713), 267 (12609), 238 (26343). FTIR (KBr disc): $\tilde{\nu}_{max}$ = 3444, 2941, 1637, 1598, 1473, 1448, 1382, 1290 cm^{-1}. MS (ESI$^+$) calcd. for C$_{13}$H$_{17}$CuN$_2$O$_3^+$; 312.0635, found 312.0590.

[Cu(*rslys*H)Cl] (2): This compound was synthesized similarly to compound **1** in which anhydrous CuCl$_2$ (0.67 g, 5.0 mmol) was used as the copper source instead of copper(II) perchlorate. Dark

bluish black crystals were obtained from a water/methanol solution mixture; yield (crystal) 69% (1.20 g). $C_{13}H_{17}N_2O_3ClCu$ (M = 348.28 g mol^{-1}): calcd. C 44.83, H 4.92, N 8.04; found C 44.94, H 4.86, N 8.05. UV/Vis [λ_{max}/nm (ε/M^{-1} cm^{-1})] (H_2O): 357 (4727), 267 (12971), 238 (27806). FTIR (KBr disc): $\tilde{\nu}_{max}$ = 3490, 2936, 1637, 1600, 1446, 1380, 1301 cm^{-1}. MS (ESI$^-$) calcd. for $C_{13}H_{16}ClCuN_2O_3^-$ 346.0245, found 346.0180.

[Cu(*slys*H)(H_2O)Cl] (3): This compound was synthesized in the same way as compound **1**, but anhydrous $CuCl_2$ (0.67 g, 5.0 mmol) was used as the copper source instead of copper perchlorate, and L-lysine (0.73, 5.0 mmol) was used instead of D/L-lysine monohydrochloride; yield (crystal) 64% (1.17 g). C, H, N analysis calcd. (%) for $C_{13}H_{19}N_2O_4ClCu$ (M = 366.30 g mol^{-1}): C 42.63, H 5.23, N 7.65; found C 42.74, H 5.26, N 7.63. UV/Vis [λ_{max}/nm (ε/M^{-1} cm^{-1})] (H_2O): 357 (3887), 267 (10429), 238 (19173). FTIR (KBr disc): $\tilde{\nu}_{max}$ = 3398, 2941, 1638, 1560, 1450, 1378 cm^{-1}. MS (ESI$^-$) calcd. for $C_{13}H_{16}ClCuN_2O_3^-$ 346.0245, found 346.0188.

[Cu_2(*rslys*H)$_2$($CH_3OH)_2$]·($H_2O)_2$($NO_3)_2$ (4): An aqueous solution of $Cu(NO_3)_2$·2.5H_2O (1.16 g, 5.00 mmol) was added to a methanolic solution of salicylaldehyde (0.50 mL, 5.0 mmol). The reaction mixture became light green. After 30 min of stirring at room temperature, an aqueous solution of D/L-lysine monohydrochloride (0.91 g, 5.0 mmol) was added dropwise to the reaction mixture, followed by the successive slow addition of a portion of aqueous $NaNO_3$ (0.55 g, 6.5 mmol). An aqueous solution of NaOH (0.2 g, 5 mmol) was then added to the reaction mixture maintained at a pH of 7–8. The reaction mixture became darker green. Then, the stirring was continued for a further 12 h. The reaction mixture was then filtered and kept for evaporation of solvent under ambient conditions. A dark green solid resulted and was washed by methanol and dried under vacuum. Green single crystals suitable for diffraction were easily obtained via recrystallization from methanol; yield (crystal) 17% (0.72 g). $C_{28}H_{46}N_6O_{16}Cu_2$ (M = 849.79 g mol^{-1}): calcd. C 39.57, H 5.46, N 9.89; found C 39.64, H 5.31, N 9.75. UV/Vis [λ_{max}/nm (ε/M^{-1} cm^{-1})] (H_2O): 357 (9381), 266 (25257), 237 (52966). FTIR (KBr disc): $\tilde{\nu}_{max}$ = 3430, 3060, 2927, 1637, 1448, 1382 cm^{-1}. MS (ESI$^+$) calcd. for $C_{26}H_{33}Cu_2N_4O_6^+$; 623.1192, found 623.0995.

[Cu_2(*slys*H)$_2$($NO_3)_2$]·($H_2O)_3$ (5): This compound was synthesized in the same manner as compound **4**, but L-lysine (0.73, 5.0 mmol) was used instead of D/L-lysine monohydrochloride; yield (crystal) 20% (0.81 g). $C_{26}H_{40}N_6O_{15}Cu_2$ (M = 803.72 g mol^{-1}): calcd. C 38.85, H, 5.02, N 10.46; found C 39.04, H 5.01, N 10.41. UV/Vis [λ_{max}/nm (ε/M^{-1} cm^{-1})] (H_2O): 357 (9875), 268 (26492), 240 (62010). FTIR (KBr disc): $\tilde{\nu}_{max}$ = 3441, 2941, 1651, 1600, 1447, 1385, 1290 cm^{-1}. MS (ESI$^+$) calcd. for $C_{26}H_{33}Cu_2N_4O_6^+$; 623.1192, found 623.0978. MS (ESI$^-$) calcd. for $C_{26}H_{32}Cu_2N_5O_9^-$; 684.0992, found 684.0468.

Crystallographic Studies: X-ray diffraction measurements were performed at 293 K with a Bruker SMART 1K CCD diffractometer using graphite-monochromated Mo-K_α radiation (λ = 0.71073 Å). Cell parameters were determined and refined by the SMART program.[17] Intensity data reduction was performed through the use of SAINT software.[17] Data were then corrected for Lorentz and polarization effects. An empirical absorption correction was applied using the SADABS program.[18] The structures were solved by direct methods using the program SHELXS-97[19] and refined by full-matrix least-squares calculations (F^2) with SHELXL-97[20] software. All non-H atoms were refined anisotropically against F^2 for all reflections. All hydrogen atoms, except for those belonging to the amine nitrogen atom (N2) and the solvent water oxygen atoms were placed at their calculated positions and refined isotropically. Hydrogen atoms attached to N2 and the water oxygen atoms (O1W, O2W and 3 W for **1**, O1W for **5**), and methanol oxygen atom were located in the difference Fourier maps and refined with isotropic displacement coefficients. In **1**, the water oxygen O4W and the perchlorate oxygen atoms (O1, O2, O3, and O4) were found crystallographically disordered over two positions. The disorders were treated using PART instructions by fixing the occupancy at 50%; the atoms were then refined isotropically. Selected bond lengths and angles are listed in Table 1. Crystal data for compounds **1**–**5** are given in Table 2.

Table 1. Comparative bond lengths and angles for compounds **1**–**5**.

Compound **1**			
O(1)–Cu(1)	1.919(17)	O(2)–Cu(1)	1.946(17)
O(1 W)–Cu(1)	1.984(2)	N(1)–Cu(1)	1.927(2)
O(1)–Cu(1)–N(1)	93.92(7)	O(1)–Cu(1)–O(1W)	89.58(8)
O(1)–Cu(1)–O(2)	177.62(7)	N(1)–Cu(1)–O(1W)	168.74(9)
N(1)–Cu(1)–O(2)	84.03(8)	O(2)–Cu(1)–O(1W)	91.94(8)
Compound **2**			
N(1)–Cu(1)	1.9435(17)	O(2)–Cu(1)	1.9453(15)
O(1)–Cu(1)	1.9169(15)	Cu(1)–Cl(1)	2.2333(7)
O(1)–Cu(1)–N(1)	92.910(7)	O(1)–Cu(1)–Cl(1)	94.04(5)
O(1)–Cu(1)–O(2)	170.60(7)	N(1)–Cu(1)–Cl(1)	170.57(6)
N(1)–Cu(1)–O(2)	83.190(7)	O(2)–Cu(1)–Cl(1)	90.84(5)
Compound **3**			
O(1)–Cu(1)	1.899(4)	O(1 W)–Cu(1)	2.356(4)
O(2)–Cu(1)	1.968(4)	Cl(1)–Cu(1)	2.3141(15)
O(1)–Cu(1)–N(1)	94.22(17)	N(1)–Cu(1)	1.946(4)
O(1)–Cu(1)–O(2)	177.66(16)	O(2)–Cu(1)–Cl(1)	92.34(11)
N(1)–Cu(1)–O(2)	83.51(17)	O(1)–Cu(1)–O(1W)	90.31(15)
O(1)–Cu(1)–Cl(1)	90.00(12)	N(1)–Cu(1)–O(1W)	97.34(15)
N(1)–Cu(1)–Cl(1)	164.78(14)	O(2)–Cu(1)–O(1W)	89.41(15)
Compound **4**			
N(1)–Cu(1)	1.9328(11)	O(2)–Cu(1)	1.9542(9)
O(1)–Cu(1)	1.9564(9)	O(4)–Cu(1)	2.3325(13)
O(1)–Cu(1)^a	1.9851(9)	Cu(1)–Cu(1)^a	3.0330(3)
N(1)–Cu(1)–O(2)	82.90(4)	O(1)–Cu(1)–O(1)^a	79.38(4)
N(1)–Cu(1)–O(1)	93.37(4)	N(1)–Cu(1)–O(4)	98.56(5)
O(2)–Cu(1)–O(1)	163.06(5)	O(2)–Cu(1)–O(4)	100.37(5)
N(1)–Cu(1)–O(1)^a	169.57(4)	O(1)–Cu(1)–O(4)	96.52(5)
O(2)–Cu(1)–O(1)^a	101.85(4)	O(1)a–Cu(1)–O(4)	89.77(5)
Compound **5**			
Cu(1)–N(1)	1.933(4)	Cu(1)–O(1)^b	1.980(3)
Cu(1)–O(1)	1.942(3)	Cu(1)–O(4)	2.311(4)
Cu(1)–O(2)	1.955(3)	O(1)–Cu(1)–O(1)^b	77.90(12)
Cu(1)–Cu(1)^b	3.0341(9)	O(2)–Cu(1)–O(1)^b	99.60(13)
N(1)–Cu(1)–O(1)	93.44(13)	N(1)–Cu(1)–O(4)	105.34(16)
N(1)–Cu(1)–O(2)	83.87(14)	O(1)–Cu(1)–O(4)	107.85(19)
O(1)–Cu(1)–O(2)	160.82(18)	O(2)–Cu(1)–O(4)	91.14(16)
N(1)–Cu(1)–O(1)^b	163.33(17)	O(1)^b–Cu(1)–O(4)	90.95(17)

Symmetry transformations used to generate equivalent atoms
a: $-x + 2, -y + 1, -z + 2$; b: $-x, y, -z + 1$

CCDC-706468 (for **1**), -706469 (for **2**), -719983 (for **3**), -719984 (for **4**) and -751598 (for **5**). These data can be obtained free of charge from The Cambridge Crystallographic Data Centre via www.ccdc.cam.ac.uk/data_request/cif.

Supporting Information (see also the footnote on the first page of this article): All types of UV/Vis, ESI mass spectra of copper(II) complexes.

Table 2. Crystal data collection and refinements data of compound **1**–**5**.

Compounds	**1**	**2**	**3**	**4**	**5**
Empirical formula	$C_{13}H_{25}N_2O_{11}ClCu$	$C_{13}H_{17}N_2O_3ClCu$	$C_{13}H_{19}N_2O_4ClCu$	$C_{28}H_{46}N_6O_{16}Cu_2$	$C_{26}H_{40}N_6O_{15}Cu_2$
FW	484.34	348.28	366.29	849.79	803.72
T /K	293(2)	293(2)	296(2)	293(2)	293(2)
Crystal system	triclinic	monoclinic	orthorhombic	triclinic	monoclinic
Space group	$P\bar{1}$	$P2_1/c$	$P2_12_12_1$	$P\bar{1}$	$C2$
a /Å	7.9147(7)	7.9786(7)	6.1671(6)	7.6836(5)	19.4951(13)
b /Å	9.0122(8)	14.0760(13)	15.5926(16)	8.9762(6)	7.8940(5)
c /Å	15.0240(12)	14.7752(13)	15.9213(14)	14.2225(9)	10.7393(7)
α /°	104.577(4)	90	90	74.339(3)	90
β /°	102.030(4)	101.570(6)	90	75.245(3)	99.053(2)
γ /°	98.638(4)	90	90	77.769(3)	90
V /Å^3	990.85(15)	1625.6(3)	1531.0(3)	902.51(10)	1632.13(18)
Z	2	4	4	1	2
$\rho_{calcd.}$ /Mgm^{-3}	1.623	1.423	1.589	1.564	1.635
μ /mm^{-1}	1.296	1.514	1.617	1.257	1.383
F(000)	502	716	756	442	832
Crystal size /mm	0.20×0.20×0.10	0.15×0.10×0.10	0.20×0.20×0.10	0.20×0.20×0.10	0.22×0.14×0.13
Reflections collected	32853	15931	9930	20039	7471
Independent reflections	7384 [R(*int*) = 0.0326]	3176 [R(*int*) = 0.0365]	2016 [R(*int*) = 0.0551]	9440 [R(*int*) = 0.0214]	2139 [R(*int*) = 0.0459]
Data/restraints/parameters	7384/5/269	3176/0/193	2016/0/190	9440/0/260	2139/1/223
GOF on F^2	1.023	1.024	0.948	1.056	1.052
$R1$,[a] $wR2$[b] [$I>2\sigma(I)$]	0.0532, 0.1573	0.0296, 0.0734	0.0302, 0.0789	0.0361, 0.0955	0.0368, 0.0836
$R1$,[a] $wR2$[b] (all data)	0.0755, 0.1824	0.0408, 0.0783	0.0406, 0.0985	0.0590, 0.1120	0.0486, 0.0902
Flack (x) parameter	–	–	0.02(3)	–	0.07(2)

[a] $R1 = (\Sigma||F_o| - |F_c||)/\Sigma|F_o|$. [b] $wR2 = \{[\Sigma(F_o^2 - F_c^2)^2]/\Sigma w(F_o^2)^2\}^{1/2}$.

Acknowledgments

D. G. C. acknowledges support from the Korea Science and Engineering Foundation (KOSEF) (grant no. R01-2008-000-12388-0) and the NRF (National Research Foundation) of Korea (Grant No. 2009-0070330). S. K. is grateful to the Korean Ministry of Education, Science & Technology for a Brain Korea 21 (BK 21) postdoctoral fellowship. We acknowledge the Korea Basic Science Institute (KBSI) for obtaining variable-temperature magnetic susceptibility measurements. We thank Teresa Linstead of the CCDC in helping deposit and update our crystallographic data.

[1] a) N. Singh, A. Singh, D. Das, M. L. Mohan, *Antioxidants Redox Signalling* **2010**, *12*, 1271–1294; b) V. C. Epa, V. A. Streltsov, J. N. Varghese, *Aust. J. Chem.* **2010**, *63*, 345–349.

[2] a) Y. H. Hung, A. I. Bush, R. A. Cherny, *J. Biol. Inorg. Chem.* **2010**, *15*, 61–76; b) P. J. Crouch, L. W. Hung, P. A. Adlard, M. Cortes, V. Lal, G. Filiz, K. A. Perez, M. Nurjono, A. Caragounis, T. Du, K. Laughton, I. Volitakis, A. I. Bush, Q. X. Li, C. L. Masters, R. Cappai, R. A. Cherny, P. S. Donnelly, A. R. White, K. J. Barnham, *Proc. Natl. Acad. Sci. USA* **2009**, *106*, 381–386; c) K. J. Barnham, A. I. Bush, *Curr. Opin. Chem. Biol.* **2008**, *12*, 222–228.

[3] a) E. Gaggelli, H. Kozłowski, D. Valensin, G. Valensin, *Chem. Rev.* **2006**, *106*, 1995–2044. See also references in: b) D. Janeš, S. Kreft, *Food Chem.* **2007**, *109*, 293–298.

[4] a) A. D. Garnovskii, A. P. Sadimenko, M. I. Sadimenko, D. A. Garnovskii, *Coord. Chem. Rev.* **1998**, *173*, 31–77; b) S. Yamada, *Coord. Chem. Rev.* **1999**, *190–192*, 537–555; c) R. L. Lieberman, A. C. Rosenzweig, *Nature* **2005**, *434*, 177–182.

[5] a) C.-M. Che, H.-L. Kwong, W.-C. Chu, K.-F. Cheng, W.-S. Lee, H.-S. Yu, C.-T. Yeung, K.-K. Cheung, *Eur. J. Inorg. Chem.* **2002**, *6*, 1456–1463; b) R. Ferreira, C. Freire, B. de Castro, A. P. Carvalho, J. Pires, M. B. de Carvalho, *Eur. J. Inorg. Chem.* **2002**, *11*, 3032–3038; c) A. Burkhardt, A. Buchholz, H. Goerls, W. Plass, *Eur. J. Inorg. Chem.* **2006**, *17*, 3400–3406; d) Y.-B. Jiang, H.-Z. Kou, R.-J. Wang, A.-L. Cui, *Eur. J. Inorg. Chem.* **2004**, 4608–4615; e) S. Thakurta, P. Roy, G. Rosair, C. J. Gómez-García, E. Garribba, S. Mitra, *Polyhedron* **2009**, *28*, 695–702; f) F. Tuna, L. Patron, Y. Journaux, M. Andruh, W. Plass, J.-C. Trombe, *J. Chem. Soc., Dalton Trans.* **1999**, 539–546.

[6] a) X. Yang, J. D. Ranford, J. J. Vittal, *Cryst. Growth Des.* **2004**, *4*, 781–788; b) R. Ganguly, B. Sreenivasulu, J. J. Vittal, *Coord. Chem. Rev.* **2008**, *252*, 1027–1050; c) M. A. Alam, R. R. Koner, A. Das, M. Nethaji, M. Ray, *Cryst. Growth Des.* **2007**, *7*, 1818–1824.

[7] a) E. M. Hodnett, P. D. Mooney, *J. Med. Chem.* **1970**, *13*, 786; b) C. A. Bolos, G. St. Nikolov, L. Ekateriniadou, A. Kortsaris, D. A. Kyriakidis, *Metal-Based Drugs* **1998**, *5*, 323–332; c) G. Plesch, C. Friebel, O. Svajlenova, J. Krätsmar-Smogrovic, D. Mlynarcik, *Inorg. Chim. Acta* **1988**, *151*, 139–143; d) G. Cerchiaro, K. Aquilano, G. Filomeni, G. Rotilio, M. R. Ciriolo, A. M. D. C. Ferreira, *J. Inorg. Biochem.* **2005**, *99*, 1433–1450; e) G. Filomeni, G. Cerchiaro, A. M. D. C. Ferreira, J. Z. Pedersen, A. De Martino, G. Rotilio, M. R. Ciriolo, *J. Biol. Chem.* **2007**, *282*, 12010–12021; f) A. T. Chaviara, E. E. Kioseoglou, A. A. Pantazaki, A. C. Tsipis, P. A. Karipidis, D. A. Kyriakidis, C. A. Bolos, *J. Inorg. Biochem.* **2008**, *102*, 1749–1764; g) V. C. da Silveira, J. S. Luz, C. C. Oliveira, I. Graziani, M. R. Ciriolo, A. M. D. C. Ferreira, *J. Inorg. Biochem.* **2008**, *102*, 1090–1103; h) P. A. N. Reddy, M. Nethaji, A. R. Chakravarty, *Eur. J. Inorg. Chem.* **2004**, *7*, 1440–1446.

[8] a) V. G. Gibson, S. K. Spitzmesser, *Chem. Rev.* **2003**, *103*, 283–316; b) S. Yamada, *Coord. Chem. Rev.* **1999**, *192*, 537–555; c) H.-B. Zhu, Z.-Y. Dai, W. Huang, K. Cui, S.-H. Gou, C.-J. Zhu, *Polyhedron* **2004**, *23*, 1131–1137; d) A. G. Dossetter, T. F. Jamison, E. N. Jacobsen, *Angew. Chem. Int. Ed.* **1999**, *38*, 2398–2400; e) J. F. Folmer-Andersen, V. M. Lynch, E. V. Anslyn, *J. Am. Chem. Soc.* **2005**, *127*, 7986–7987; f) S. Khatua, K. Kim, J. Kang, J. O. Huh, C. S. Hong, D. G. Churchill, *Eur. J. Inorg. Chem.* **2009**, 3266–3274.

[9] a) S. Khatua, S. H. Choi, J. Lee, K. Kim, Y. Do, D. G. Churchill, *Inorg. Chem.* **2009**, *48*, 2993–2999; b) S. Khatua, J. Kang, J. O. Huh, C. S. Hong, D. G. Churchill, *Cryst. Growth Des.* **2010**, *10*, 327–334; c) S. Khatua, J. Kang, D. G. Churchill, *New J. Chem.* **2010**, *34*, 1163–1169.

[10] A. W. Addison, T. N. Rao, J. Reedijk, J. van Rijn, G. C. Verschoor, *J. Chem. Soc., Dalton Trans.* **1984**, *7*, 1349–1356.
[11] D. G. Churchill, *J. Chem. Educ.* **2006**, *83*, 1798–1803.
[12] S. Khatua, S. H. Choi, J. Lee, J. O. Huh, Y. Do, D. G. Churchill, *Inorg. Chem.* **2009**, *48*, 1799–1801.
[13] a) C.-T. Yang, M. Vetrichelvan, X. Yang, B. Moubaraki, K. S. Murray, J. J. Vittal, *Dalton Trans.* **2004**, 113–121; b) X. Wang, J. Ding, J. J. Vittal, *Inorg. Chim. Acta* **2006**, *359*, 3481–3490; c) S. M. Couchman, J. C. Jeffery, P. Thornton, M. D. Ward, *J. Chem. Soc., Dalton Trans.* **1998**, 1163–1169; d) V. K. Muppidi, S. Pal, *Eur. J. Inorg. Chem.* **2006**, *14*, 2871–2877.
[14] The *g* value for **4** is somewhat smaller than the usual ones for Cu^{II} complexes. However, the identical *g* parameters were also found in similar Cu^{II} dimeric systems [Sehadrinarayan Khatua, Kibong Kim, Jina Kang, Jung Oh Huh, Chang-Seop Hong, David G. Churchill, *Eur. J. Inorg. Chem.* **2009**, 3266–3274]. The fraction of noncoupled species was rather higher than expected, even though we measured magnetic data with seemingly analytically pure samples, probably indicating a significant degree of paramagnetic impurities existing in these materials.
[15] a) L. Rodriguez, E. Labisbal, A. Sousa-Pedrares, J. A. Garcia-Vazquez, J. Romero, M. L. Duran, J. A. Real, A. Sousa, *Inorg. Chem.* **2006**, *45*, 7903–7914; b) B. Sreenivasulu, F. Zhao, S. Gao, J. J. Vittal, *Eur. J. Inorg. Chem.* **2006**, 2656–2670; c) S. Khatua, K. Kim, J. Kang, J. O. Huh, C. S. Hong, D. G. Churchill, *Eur. J. Inorg. Chem.* **2009**, 3266–3274.
[16] W. H. Crawford, H. W. Richardson, J. R. Wasson, D. J. Hodgson, W. E. Hatfield, *Inorg. Chem.* **1976**, *15*, 2107–2110.
[17] *SMART* and *SAINT*, *Area Detector Software Package and SAX Area Detector Integration Program*, Bruker Analytical X-ray, Madison, WI, **1997**.
[18] *SADABS*, Area Detector Absorption Correction Program, Bruker Analytical X-ray, Madison, WI, **1997**.
[19] SHELXS-97, *Program for Crystal Structure Determination*, G. M. Sheldrick, *Acta Crystallogr., Sect. A* **1990**, *46*, 467–473.
[20] a) G. M. Sheldrick, **1999**, *SHELXL-97*, *Program for Crystal Structure Solution and Refinements*, University of Göttingen, Göttingen, Germany; b) G. M. Sheldrick, *Acta Crystallogr., Sect. A* **2008**, *64*, 112–122.

Received: May 20, 2010
Published Online: September 17, 2010

